

Fabrication and optical characterization of a high-quality fcc-opal-based photonic crystal grown by the vertical convective self-assembly method

Octavio Alejandro Castañeda-Uribe^{1,3}, Juan Carlos Salcedo-Reyes*¹, Henry Alberto Méndez-Pinzón¹,
Aura Marina Pedroza-Rodríguez²

¹Grupo de Películas Delgadas, Departamento de Física. ²Grupo de Biotecnología Ambiental e Industrial (GBAI), Departamento de Microbiología, Facultad de Ciencias. ³Departamento de Ingeniería Electrónica. Pontificia Universidad Javeriana, Bogotá, D.C., Colombia.

*salcedo.juan@javeriana.edu.co

Received: 18-06-2010; Accepted: 15-07-2010

Abstract

Objective: Fabrication and optical characterization of close-packed 225 nm SiO₂-based colloidal crystals. **Materials and methods:** The vertical convective self-assembly method is used to grow high-quality 225 nm close-packed SiO₂-based colloidal crystals. An annealing process (550°C) is made in order to improve the mechanical stability of the sample. Optical characterization is done by angle-resolved transmission spectroscopy (A-RTS) and structural characterization by Scanning Electron Microscopy (SEM). **Results:** Both, A-RTS and SEM, show that with the vertical convective self-assembly method, with the appropriate parameters of temperature of evaporation (60°C), volume fraction of the colloidal suspension (0.2% w/w) and acidity (pH=6), highly ordered close packed face centered cubic (fcc) SiO₂ based colloidal crystals are obtained. **Conclusions:** The growth of high-quality (long range order and defect-free) face centered cubic opal-based photonic crystals is reported.

Key words: Photonic crystals, colloidal crystals, artificial opals, vertical convective deposition method, Bragg diffraction

Resumen

Fabricación y caracterización óptica de cristales coloidales de alta calidad formados por esferas de SiO₂ de 225 nm de diámetro con empaquetamiento fcc crecidos por el método convectivo de auto-ensamblado de deposición vertical. **Objetivo:** Fabricación y caracterización óptica de cristales coloidales de esferas de SiO₂ de 225 nm de diámetro y empaquetamiento fcc. **Materiales y métodos:** Se producen cristales coloidales de 225 nm de diámetro de alta calidad mediante la técnica convectiva de auto-ensamblado de deposición vertical. Se hace, adicionalmente, un proceso de recocido (550°C) con el fin de mejorar la estabilidad mecánica de la estructura. La caracterización óptica se lleva a cabo por espectroscopia de transmisión resuelta en ángulo (A-RTS) y la caracterización estructural mediante microscopía electrónica de barrido (SEM). **Resultados:** Ambos, A-RTS y MEB, muestran que con el método utilizado y con los parámetros adecuados de temperatura de evaporación (60°C), fracción en volumen de la suspensión coloidal (0,2% w / w) y acidez (pH = 6) se obtienen cristales coloidales de SiO₂ con empaquetamiento compacto fcc altamente ordenados. **Conclusiones:** Se reporta el crecimiento de ópalo artificiales con empaquetamiento compacto fcc altamente ordenados (libre de defectos y con ordenamiento a largo alcance).

Palabras clave: Cristales fotónicos, cristales coloidales, ópalo artificiales, método de deposición vertical, difracción de Bragg

Resumo

Fabricação e caracterização óptica de cristais coloidais de alta qualidade formados por esferas de SiO₂ de 225 nm de diâmetro com embalagem fcc crescidos pelo método convectivo de automontagem de deposição vertical. Objetivo: Fabricação e caracterização óptica de cristais coloidais de esferas de SiO₂ de 225 nm de diâmetro e embalagem fcc. **Materiais e métodos:** Foram produzidos cristais coloidais de 225 nm de diâmetro de alta qualidade através da técnica convectiva de automontagem de deposição vertical. Faz-se, adicionalmente, um processo de recozimento (550°C), a fim de melhorar a estabilidade mecânica da estrutura. A caracterização óptica foi realizada por espectroscopia de transmissão em ângulo (A-RTS) e a caracterização estrutural utilizando microscopia eletrônica de varredura (MEV). **Resultados:** Ambos, A-RTS e MEV mostram que com o método utilizado e com os parâmetros adequados de temperatura de evaporação (60°C), fração de volume da suspensão coloidal (0,2% w / w) e acidez (pH = 6) são obtidos cristais coloidais de SiO₂ com embalagem compacto fcc altamente ordenados. **Conclusões:** Registrou-se o crescimento de opalas artificiais com embalagem compacto fcc altamente ordenadas (livres de defeitos e de ordem de longo alcance).

Palavras-chave: cristais fotônicos, cristais coloidais, opalas artificiais, método de deposição vertical, difração de Bragg

Introduction

Photonic meta-materials, artificially engineered materials in which their optical properties are unattainable with naturally occurring materials, attract a great deal of attention mainly because of their ability to control the way in which the electromagnetic radiation interacts with them and, also, because they represent one of the most important examples of the so-called emerging technologies in the fields of electronics and optoelectronics (1). A particular kind of photonic meta-materials are the close-packed 3D colloidal crystals: periodic arrangement (face centered cubic (fcc) and/or hexagonal close packed (hcp) stacking lattice) of mono-disperse silica or polystyrene nano-spheres with diameters within the wavelength range of visible light in which many novel optical phenomena, that are strongly dependent of the sphere-packing symmetry, are observed (2). One of the most important optical characteristics in a SiO₂-based colloidal crystal, which can be detected directly by the A-RTS, is the presence of stop bands in which propagation of light is allowed only in certain crystallographic directions. Scattering of light, therefore, follows the Bragg's law, in the same sense that X-rays are diffracted by a family of planes of the atomic crystals. These novel optical phenomena foster a great number of potential applications in advanced optical devices such as waveguides (3), sensors (4), lenses (5) and low threshold lasers (6,7).

Although the detailed growth mechanism of these colloidal crystals is not known (8), upon both thermodynamic studies and experimental results it is well known that under the appropriate conditions, colloidal particles assemble spontaneously into ordered structures (9), giving place to the called self-assembly methods. Although numerous self-assembly methods have been employed to make such 3D colloidal crystals (sedimentation (10,11), electrophoresis (12), and spin coating (13), mainly), the low control over the growth parameters results in a variety of defects in such

a way that the controlled and uniform growth of 3D colloidal crystals remained to be developed. However, the controlled evaporation-induced self-assembly vertical deposition method, in which capillary forces produce large high-ordered opal films due to the directional nature of the substrate/colloidal suspension interface, has shown to be one of the more efficient methods (14, 15).

The present work reports the growth of long-ordered 225 nm fcc-SiO₂-based colloidal crystals from self-assembly vertical deposition method on a hydrophilic glass substrate, evaporation temperature of 60°C, volume fraction of the colloidal suspension of 0.2% w/w, pH of 6 and annealing of 550C. The paper is organized as follows. In section 2 the experimental details (materials, instrumentation and procedures) are presented. In section 3, a structural analysis from the SEM images of the structure is provided. Optical properties, from A-RTS, of the opal films will be obtained showing the existence of a stop band, typical in the optical behavior of light in photonic crystals, which follows the Bragg's law.

Materials and methods

Mono-disperse colloidal SiO₂ spheres with a nominal diameter of 250nm (Ångström Spheres® 0.25 μm silica spheres: SIOP025-01-100G) were assembled on a soda lime float glass substrate (Knittel standard microscope slides) by self-assembly vertical deposition. The glass substrate was cleaned ultrasonically with acetone (Merck, GR for analysis), ethanol (Merck, absolute GR for analysis), and fully rinsed with deionized water (Milli-Q water, 0.056 μS·cm⁻¹) followed by drying under a flow of nitrogen gas before use. In order to make the surface hydrophilic, the glass substrate was etched by immersion in piranha solution (a solution containing sulfuric acid (Merck H₂SO₄,

95-97%) and hydrogen peroxide (Carlo Erba H_2O_2 , solution 30% m/m in water) of 3:1 in volume) for 30 min followed by rinsing with deionized water and dried with nitrogen. The hydrophilic substrate was immersed vertically into a vial (25mL) containing a diluted solution of SiO_2 spheres, used as received from the supplier (Ångström Spheres®), of 0.2% w/w in 20mL of deionized water. The acidity of the solution was controlled by using adequate amounts of chlorohydric acid (HCl) and Sodium hydroxide (NaOH) in order to obtain a pH of 6.

The vial was then placed in a vibration-free temperature controlled chamber (Terrigeno furnace mod. L2) programmed to heat at 60°C for 25h. Two type K thermocouples were placed into the chamber in order to monitor the distribution and eventual changes of temperatures over the time as in figure 1. Thermocouple 1 was in the air, T_{ref} in figure 1, and thermocouple 2 was dipping in the suspension, T in figure 1. Finally the deposited film was annealed at 550°C for 2h (Terrigeno furnace Mod. L2) in order to improve the mechanical stability of the sample.

Optical properties, which determine the presence of a stop band in the dispersion relation of the structure, were studied by means of A-RTS measurements in the UV-Visible range. The impinging light (Newport 6333 Quartz Halogen Lamp) was focused to a spot of 3.0mm², the transmitted light was collected by a monochromator (Acton

research spectral pro 775), detected by a photomultiplier tube (77342 Side-on Oriel PMT) and sent to a Lock-in amplifier (Stanford Research Systems SR830). Scanning Electron Microscope (SEM) was used to carry out a structural characterization of the sample (JEOL, Mod. JSM 6490-LV operated at 20 kV). The sample was coated with gold to enhance the conductivity and avoid possible charging.

Results and discussion

In the convective self-assembly method the weakly interacting SiO_2 colloidal spheres are crystallized near the moving contact line between the stationary substrate and the concave meniscus formed between the surface of the very low concentrated evaporating suspension and the hydrophilic substrate (**Figure 1**). The convective flow of solvent (deionized water in this case) through the interstitial sites induces lateral capillary forces that in turn cause an attractive interaction between the spheres in such a way that are pushed to the flat substrate, just as in the case of the dip coating technique (16). In general, there are many types of interactions between the spheres (mainly Van der Waals, Brownian and Coulomb interactions), however the capillary forces acting between the colloidal spheres are larger compared with them. For this reason, convective methods are sometimes known as self-assembly by capillary forces (17).

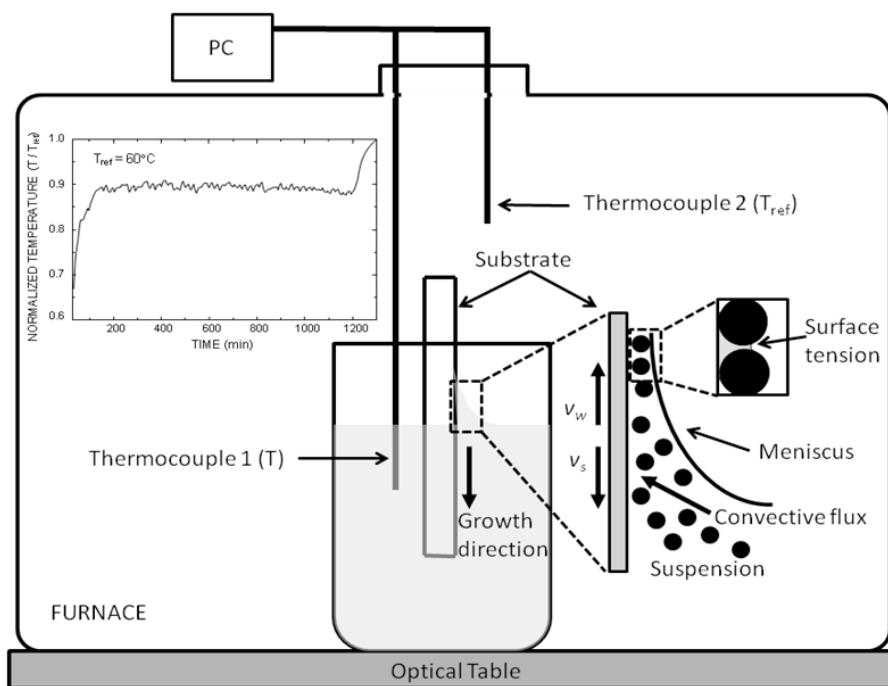


Figure 1. Schematic diagram of the vertical convective self-assembly setup. The inset shows the solvent temperature at $T_{ref}=60^{\circ}C$. The water and spheres fluxes in the vicinity of the hydrophilic substrate as well as the surface tension are shown.

The convective transfer of SiO_2 spheres from the solution to the hydrophilic substrate is forced primarily by the temperature dependent solvent evaporation. Taking into account that there is not a thermodynamic equilibrium between the solvent vapor pressure and the solution surface and supposing mechanical equilibrium, the solvent evaporation produces a pressure gradient that is compensated by a solvent influx from the bulk solution and a sphere flux that causes the accumulation of particles in the substrate, forming a disordered dense mono-layer. Then capillary pressure due to curvature of the liquid surface between neighboring spheres lead to specific crystallization during the dried process. One of the most important facts in the growth of high quality films by convective methods is the constancy of the particle volume fraction in the meniscus area that depends mainly of the sedimentation velocity (described by the Kynch theory (18)) and the solvent evaporation rate (v_s and v_w in figure 1, respectively). Due to that, the phase change of a solvent from its free surface occurs only under non-equilibrium conditions, the vertical convective method is a system that is not in thermodynamic equilibrium and, consequently, the parameters that govern the growth process were not completely understood. However, it is well known that if the environmental conditions like the suspension evaporation rate, the particle sedimentation velocity, the particle volume fraction in the solution and the shape of the meniscus are properly controlled, a thin film of (fcc/hcp) close-packed

colloidal spheres is deposited on the substrate as the meniscus moves down it (19). Both stacking patterns (fcc and hcp) have identical packing densities ($\frac{\pi\sqrt{2}}{6} = 74\%$) and coordination numbers (twelve). This is why, within the framework of photonic applications, the impact of the morphology on the optical properties of self-assembled colloidal crystals draws a lot of interest. From theoretical calculations (20), both structures are energetically similar, that is, the free energies (per particle) are the same within an uncertainty of no more than $2 \times 10^{-3} K_B T$ (21).

In figure 2 the classical ABC notation is used to denote each possible position of the hexagonal close packed mono-layer (22): A, B (displaced by $(r, r\sqrt{3}/3, 0)$ from A), and C (displaced by $(2r, 2r\sqrt{3}/3, 0)$ from A), where r is the radius of the spheres. In all cases the displacement is referred to the i, j, k unit vectors that define the coordinate system. If the stacking sequence is regular, the arrangement of spheres grown may be a [111]-fcc structure, with a repeated ABCABC... pattern (every third layer is the same), or a [001]-hcp structure, with a repeated ABAB... pattern (every other layer is the same) (23, 24). The generic systems are described in figure 2. The [001]-hcp structure is shown, in a perpendicular view to the (100) plane, in figure 2a and the [111]-fcc structure is shown, in a projection perpendicular to the (111) plane, in figure 2b. The primitive vectors $a_1, a_2,$ and $a_3,$ and the primitive cells are also shown.

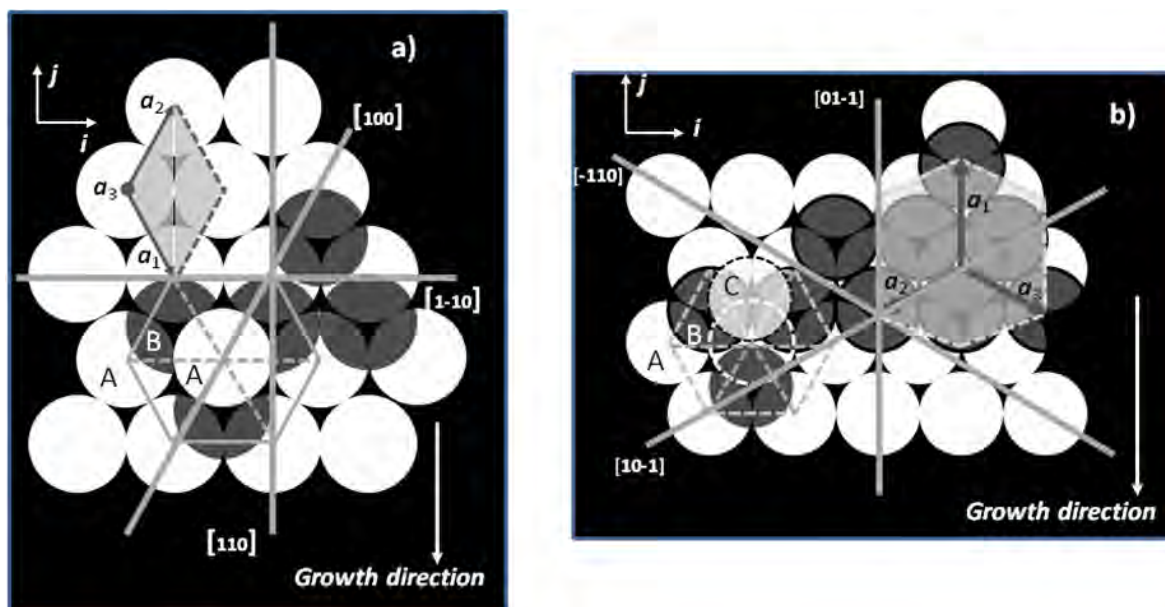


Figure 2. Schematic diagram of the [001]-hcp (a) and [111]-fcc (b) stacking pattern on mono-disperse spheres in a perpendicular view to the growth direction. The primitive vectors (a_1, a_2, a_3) and the primitive cell are shown in each case.

A typical scanning electron microscope (SEM) image of the SiO₂ opal-based photonic crystal made by the vertical convective self-assembly method at a growth temperature of 60°C, volume fraction of the colloidal suspension of 0.2% w/w, pH of 6 and annealing temperature of 550°C is shown in figure 3. The top surface (parallel to the substrate) of a high quality micro-colloidal crystal composed of 225 nm SiO₂ spheres with a distribution standard deviation less than 6% (Figure 3) assembled in a hexagonally close-packed ordered array is observed. In figure 3 the *i* direction (row of spheres) is parallel to the growth direc-

tion of the crystal. From figure 2, at least three layers (ABC for fcc or ABA for hcp) must be considered in order to establish the 3D colloidal stacking pattern. In figure 4 a four layer top view SEM image (Figure 4a) is compared with a [111]-fcc stacking lattice model (Figure 4b). The ABCA pattern is observed indicating clearly that the colloidal crystal has a cubic structure. Confirming this result, figure 5a gives a cross-sectional view of the sample and figure 5b a simulation that shows the [01-1] direction of an fcc lattice. From figure 5 a [111]-fcc-stacking lattice of high quality with uniform thickness of 6.5µm is observed.

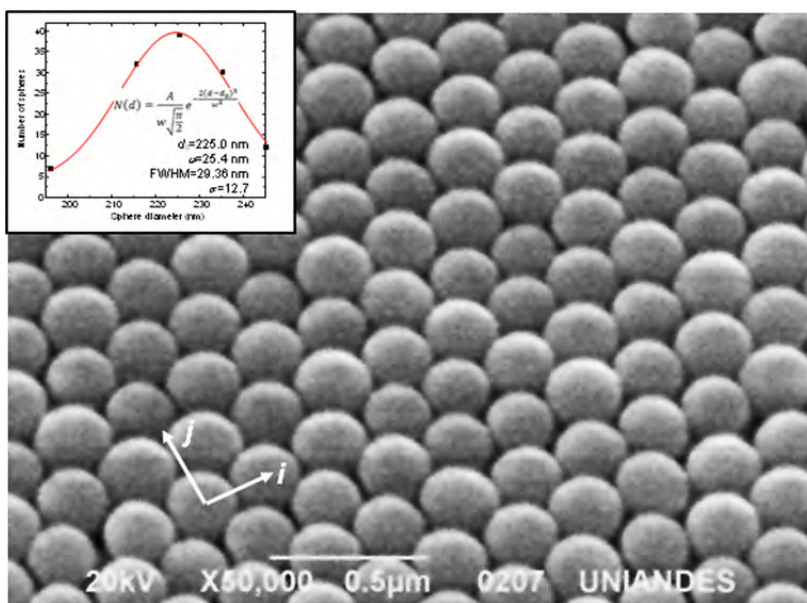


Figure 3. SEM image of a 230 nm fcc-SiO₂ opal based photonic crystal grown by the self-assembly convective vertical deposition method. The inset shows the dispersion of the diameter of the spheres.

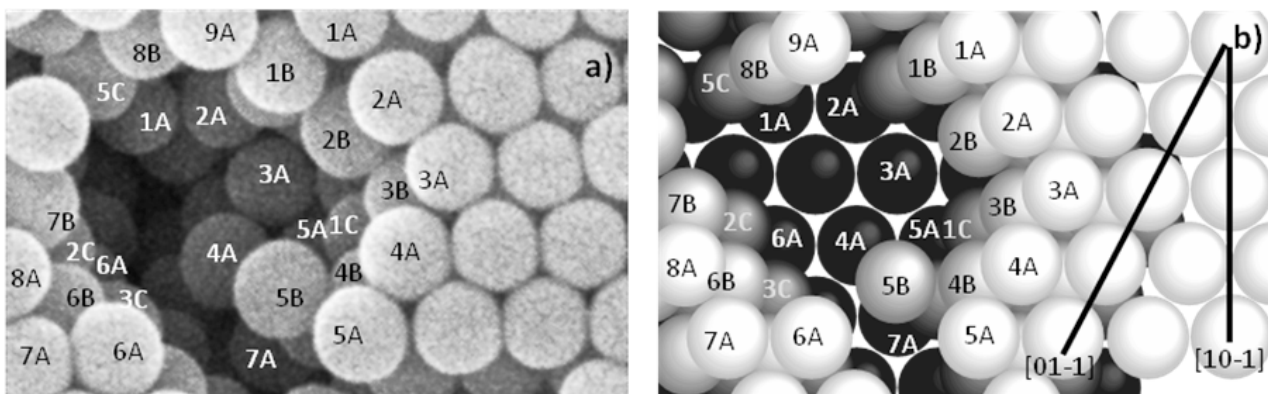


Figure 4. a) A perpendicular SEM image of a 230 nm SiO₂ based colloidal crystal. b) Computer simulation of an fcc stacking lattice that has been trimmed to show the arrangements of spheres similar to those observed in a). The letters (ABCA...) show the stacking pattern typical of an fcc structure.

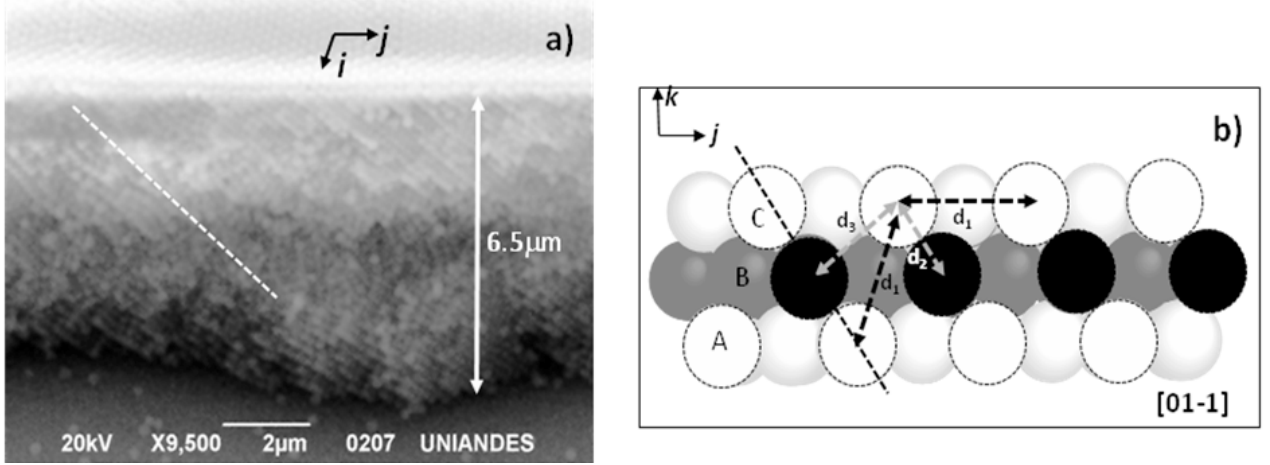


Figure 5. a) SEM image of the cleaved facets. b) Computer simulation of the (01-1) plane of an fcc stacking lattice, where $d_1 = 2r\sqrt{3}$, $d_2 = 2r$, $d_3 = 2r\sqrt{2}$, and $d_4 = 2r\sqrt{(8/3)}$. The white dashed line in a) corresponds to the black dashed line in b).

In order to investigate the angular-dependent spectral response of the transmitted intensity under excitation with visible light, in which the direction of the specular reflection of light from the sample surface and the direction of diffraction from the colloidal crystal coincide, of the 225 nm SiO₂ opal-based colloidal crystal, under the assumption of a perfect fcc stacking lattice, the Bragg formulation of diffraction is used. Since the wavelength of visible light (350-800 nm) is close to the lattice constant ($a_0 = 2\sqrt{2}r \sim 350$ nm, for spheres with diameter of 250 nm), the geometry of the diffraction conditions is very similar to the one that occurs in X-ray diffraction by an atomic crystal in which, for certain sharply defined wavelengths and incident directions, intense peaks (first order Bragg peaks) of scattered radiation are observed due to the interaction of light with a periodic dielectric permittivity. In the Bragg description of the diffraction of radiation by a crystal, two assumptions are made: *i*) Radiation is specularly reflected by a family of planes in the structure and *ii*) the reflected rays interfere constructively when the condition

$$\lambda_{max} = 2d \sqrt{n_{eff}^2 - \sin^2\theta} \quad [1]$$

is satisfied, where λ_{max} is the wavelength of the first-order diffraction peak, d is the distance between reflecting adjacent planes ([111] planes for an fcc structure with $d = \frac{4}{\sqrt{6}}r$ and [001] planes for a hcp structure with $d = \sqrt{\frac{8}{3}}r$), θ is the angle between the incident light beam and the normal to the surface of the sample ([111] direction for fcc and [001] direction for hcp) and n_{eff} is the effective refractive index of the material

$$n_{eff} = \sqrt{n_{SiO_2}^2 * f_{SiO_2} + n_{air}^2 * f_{air}} \sim 1.34 \quad [2]$$

where n_{SiO_2} is the refractive index of the SiO₂ ($n_{SiO_2} = 1.45$, for silica bulk), n_{air} is the refractive index of air ($n_{air} = 1.0$), f_{SiO_2} is the filling factor of the silica ($f_{SiO_2} = \frac{2\sqrt{2}\pi}{6} = 74\%$, for both, fcc and hcp structures) and f_{air} is the filling factor of the voids ($f_{air} = 26\%$). Due to the fact that inter-planar distances (distance between [111] planes in fcc and between [001] planes in hcp) are the same in both stacking lattices ($d = \sqrt{\frac{8}{3}}r$), it is clear that the determination of an fcc or hcp stacking lattice cannot be done from the Bragg's formula. However, from figures 5 and 6 an fcc-stacking lattice can be deduced.

When non polarized light with wavelength of 450-650 nm impinges parallel to the surface of the substrate (the [111] direction of the 225 nm fcc-SiO₂ based photonic crystal, as is shown in figure 2) a strong absorption band, a narrow photonic stop band, centered on 505 nm and with a Full-Width at Half-Maximum (FWHM) of 40 nm is observed (**Figure 6**) in contrast with the transmittance spectrum of amorphous SiO₂ (sample grown at a temperature of 60°C, volume fraction of the colloidal suspension of 0.1% w/w, pH of 9 and annealing temperature of 550°C in which ordering was not observed). Following the Bragg's law, the wavelength of the stop band can be tuned by tilting the {111} surface of the colloidal crystal relative to the incident light. The wavelength (λ_{max}) of the first-order diffraction peak as a function of the incidence angle is shown in

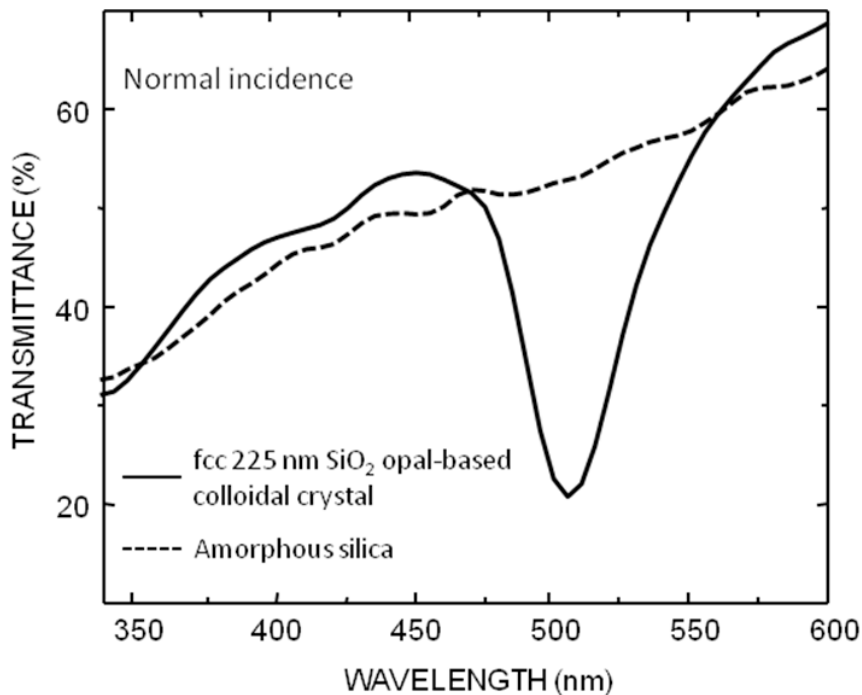


Figure 6. UV-VIS transmission spectra of the film measured with the incident light normal to the substrate. A narrow first-order diffraction peak is observed, in contrast with the spectra of an amorphous SiO₂ sample.

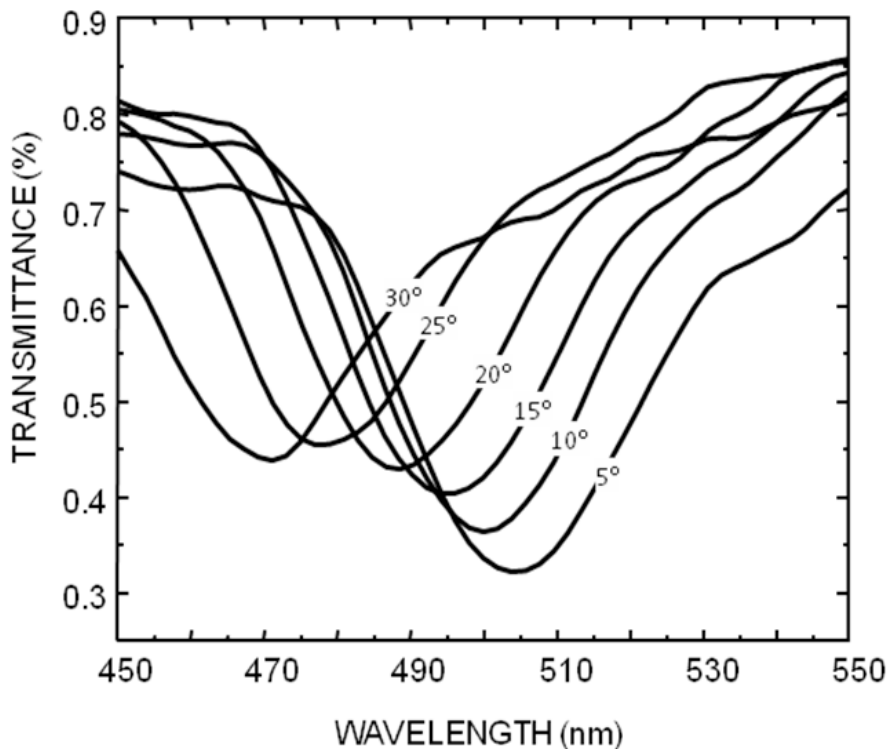


Figure 7. UV-VIS Angle-resolved transmission spectra of the film measured with the incident light forming an angle ϕ respect to the normal of the substrate.

figure 6 by means of the angle-resolved transmission spectra, and a plot of $\sin^2(\phi)$ vs λ^2 following the Bragg equation is shown in figure 7. From a linear fit to the experimental data, the values $n_{\text{eff}} = 1.34 \pm 0.5\%$ and $r = 115 \text{ nm} \pm 1\%$ are obtained in extremely high agreement with the theoretical value of the effective refractive index and, on the other hand, with the measurement of the diameter of the spheres done by SEM (Figure 3).

Conclusions

Fabrication of high quality 230 nm fcc-SiO₂ opal based photonic crystals by the vertical convective self-assembly method is reported with the following growth parameters: volume fraction = 0.2%, pH = 6, evaporation temperature = 60°C, and annealing temperature = 550°C for 2 hours. SEM images of different areas of the film show that the stacking pattern is fcc. However, there are several observed imperfections of the film such as: point defects, dislocations and cracks. The particle size obtained using the Bragg condition is in excellent agree-

ment with the particle size measured by SEM as well as the effective refractive index.

Acknowledgments

We are grateful to Dery Esmeralda Corredor at the MEB Characterization Laboratory of the Universidad de los Andes (Bogotá, Colombia).

Financial support

Work partially supported by OFI-PUJ (Oficina para el Fomento de la Investigación de la Pontificia Universidad Javeriana) under grant 003385 and by “Fundación para la Promoción de la Investigación y la Tecnología, Banco de la República de Colombia” under grant 200904.

Conflict of interest

There is no conflict of interest on the type of devices or procedures described in this manuscript.

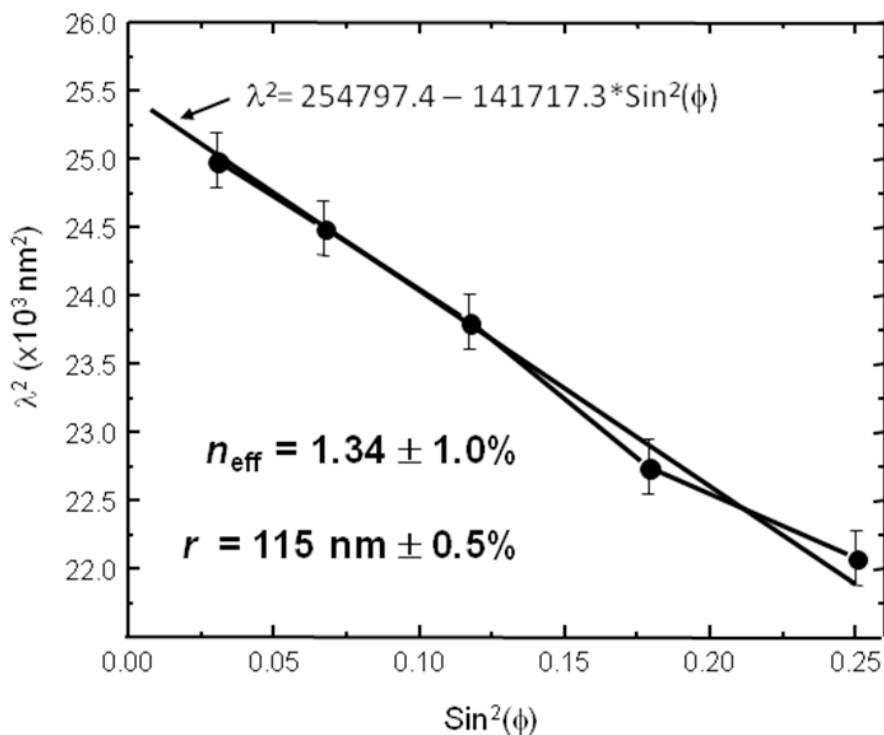


Figure 8. Plot of $\sin^2(\phi)$ as a function of λ^2 based on Bragg's equation. The straight line is the linear fit of the experimental data (circles).

References

1. Boltasseva, A., and Shalaev, V. M. "Fabrication of optical negative-index metamaterials: recent advances and outlook". *Metamaterials*. 2008; **2**: 1-17
2. Salcedo-Reyes J.C. "Refraction properties of fcc and hcp SiO₂-based colloidal crystals". *Proceeding of SPIE*. 2010; **7609**: 76091K
3. Tandon S.N., Soljagic M., Petrich G. S., Joannopoulos J. D., Kolodziejski L. A. The superprism effect using large area 2D-periodic photonic crystal slabs. *Photonics and Nanostructures-Fundamentals and Application.*, 2005; **3**: 10-18.
4. Nair R. V., Vijaya R. Photonic crystal sensors: An overview. *Progress in Quantum Electronics*. 2010; Article in press.
5. Srivastava R., Thapa K. B., Pati S., Ojha S. P. Negative refraction in 1D photonic crystals. *Solid State Communications*. 2008; **147**: 157-160.
6. Özbat E., Michel E., Tuttle G., Biswas R., Sigalas M. M., Ho K. M. Micromachined millimeter-wave photonic band-gap crystals. *Applied Physics Letters*. 1994; **64**: 2050-2061.
7. Busch K, von Freymann G, Linden S, Mingaleev SF, Tkeshelashvili L, Wegener M. Periodic nanostructures for photonics. *Physics Reports*. 2007; **444**: 101-202.
8. Norris D. J., Arlinghaus E. G., Meng L., Heiny R., Scriven L. E., Opaline Photonic Crystals: How Does Self-Assembly Work?. *Advanced Materials*. 2004; **16**: 1393-1399.
9. Woodcock L. V. Entropy difference between the face-centred cubic and hexagonal close-packed crystal structures. *Nature*. 1997; **385**: 141-143.
10. Liao L, Huang Y. Process optimization of sedimentation self-assembly of opal photonic crystals under relative humidity-controlled environments. *Expert Systems with Applications*. 2008; **35**: 887-893.
11. Zhou Q, Dong P, Liu L, Cheng B. Study on the sedimentation self-assembly of colloidal SiO₂ particles under gravitational field. *Colloids and Surfaces A*. 2005; **253**: 169-174.
12. Chung Y. W., Leu I. C., Lee J. H., Hona M. H. Fabrication and characterization of photonic crystals from colloidal processes. *Journal of Crystal Growth*. 2005; **275**: e2389-e2394.
13. Jiang P., McFerland M. J. Large-Scale Fabrication of Wafer-Size Colloidal Crystals: Macroporous Polymers and Nanocomposites by Spin-Coating. *Journal of the American Chemistry Society*. 2004; **126**: 13778–13786
14. Jiang P., Bertone J. F., Hwang K. S., Colvin V. L. Single-crystal colloidal multilayers of controlled thickness. *Chemistry of Materials*. 1999; **11**: 2132-2140.
15. Teh, L. K., Tan N. K., Wong C. C., Li S. Growth imperfections in three-dimensional colloidal self-assembly. *Applied Physics A*, 2005; **81**: 1399-1404
16. Pallavidino L., Santamaria Razoza D., Geobaldo F., Balestrerib A., Bajonib D., Gallib M., Andreanib L.C., Ricciardic C., Celascoc E., Quaglioc M., M. Giorgisc M. Synthesis, characterization and modelling of silicon based opals. *Journal of Non-Crystalline Solids*. 2006; **352**: 1425-1429.
17. Dimitrov A. S., Nagayama K. Continuous convective assembling of fine particles into morphocolored two-dimensional arrays. *Langmuir*. 1996; **12**: 1303–1311.
18. Kynch, G. J. A. Theory of Sedimentation. *Transactions of the Faraday Society*. 1925; **48**: 166-176.
19. Checoury X., Enoch, S., López, C., and Blanco, A. Stacking patterns in self-assembly opal photonic crystals. *Applied Physics Letters*. 2007; **90**:161131
20. Woodcock L. V. Entropy difference between the face-centred cubic and hexagonal close-packed crystal structures. *Nature*. 1997; **385**: 141-143.
21. Pusey P. N., van Megen W., Barlett P., Ackerson B. J., Rarity J. G., Underwood S. M. Structure of crystals of hard colloidal spheres. *Physical Review Letters*. 1989; **63**: 2753-2756.
22. Pandey D., Krishna P. *International Tables for Crystallography*. Vol. C, Section 9.2.1.1 International Union of Crystallography. 2006; 752p.
23. Ashcroft N. W., Mermin N.D. *Solid State Physics*. Harcourt College Publishers, New York, USA. 1976: 826p.
24. Pandey D., Krishna P. Polytypism in close-packed structures, *Current Topics in Materials Science*. 1982; **9**: 415-491.